Pharmacogenomics and Personalized Medicine

Dovepress

open access to scientific and medical research

Open Access Full Text Article

ORIGINAL RESEARCH

TICRR Overexpression Enhances Disease Aggressiveness and Immune Infiltration of Cutaneous Melanoma

Cheng Chen, Yong Zou, Xiangbing Zheng, Taotao Hu, Jie Ni, Daohong Kan, Zongyin Yin, Lingxiao Ye, Bing Liu

Department of Burn and Plastic Surgery, The Second People's Hospital of Yibin (West China Yibin Hospital, Sichuan University), Yibin, Sichuan, People's Republic of China

Correspondence: Bing Liu, Email 4444093330@qq.com

Objective: To investigate the role of the TopBP1 interacting checkpoint and replication regulator (TICRR) in cutaneous melanoma (CM) as a prognostic biomarker and therapeutic target.

Methods: TICRR expression in tumour samples was explored using the TCGA and the GTEx database. The Kaplan-Meier survival curve, nomogram model and risk score curve were established to evaluate the prognostic role of TICRR in CM. Tissue samples of CM patients were obtained to validate the TICRR expression further. Several experiments in vitro were conducted to investigate the effect of TICRR upon CM aggressiveness and to explore underlying mechanisms.

Results: TICRR was overexpressed in CM tissue and was correlated with poor prognosis of CM patients. The knockdown of TICRR decreased the proliferation, migration, and invasion of CM cells, whereas overexpression produced the opposite effect. Furthermore, TICRR suppression substantially attenuated the activation of PI3K/AKT/mTOR signalling, while the PI3K/AKT inhibitor LY294002 could partially reverse the aggressiveness-enhancing effect induced by TICRR overexpression. It was further confirmed that TICRR was closely related to immune cell infiltration activities by using immune infiltration and immunofluorescence analysis.

Conclusion: TICRR overexpression may enhance CM aggressiveness by activating the PI3K/Akt/mTOR pathway and promoting immune infiltration. TICRR was verified as a potential prognostic biomarker and therapeutic target for CM.

Keywords: cutaneous melanoma, TICRR, immune infiltration, invasion, prognosis

Introduction

Cutaneous melanoma (CM), the most aggressive skin cancer emerging from pigmented melanocytes, is a great concern for public health worldwide due to its increasing incidence and alarming mortality.[1] Although the risk generally escalates with age and the incidence is higher among older populations, CM is among the most common cancers in young adults, placing an immense burden on individuals, families, and society.[2,3] In recent years, more and more researchers have paid attention to the association between molecular biomarkers and the development or progression of CM and shed light on their roles in diagnosing and treating the disease.[4–6] Several biomarkers, such as S100, HMB45, PRAME, BRAF V600E and Ki-67, have been checked and validated with reliable confidence. Specifically, some can aid in detecting and subtyping melanoma, some for assessing metastatic lesions and some for predicting prognosis.[2,7] Due to the extraordinarily heterogeneous histopathological of CM, immunohistochemical, and molecular landscape, few existing markers satisfied both clinical diagnosis and treatment needs. Therefore, more novel prognostic biomarkers and therapeutic targets are needed to improve the understanding of the pathogenesis and management of this fatal disease.

The replication of eukaryotic DNA is strictly regulated to ensure the complete replication of the genome in each cell cycle.[8] Malignancies, characterised by rapid cell proliferation, require DNA hyper-replication, which can result in genomic instability and accelerate tumour development.[9] TopBP1-interacting checkpoint and replication regulator

Received: 21 March 2024
Accepted: 26 August 2024
Published: 3 September 2024

(TICRR), as a regulator of DNA replication, is involved in initiating DNA replication via its interaction with TopBP1.[10] Overexpression of TICRR has been reported to be involved in tumorigenesis, chemotherapy resistance, and poor clinical outcomes.[11,12] TICRR has emerged as a viable therapeutic target and a reliable prognostic indicator in lung adenocarcinoma, hepatocellular carcinoma and renal cell carcinoma, with implications in immune activation, cell cycle regulation, RNA modification, and tumour energy metabolism.[12–14] However, the expression of TICRR and its potential role in CM has yet to be elucidated. Given this, the clinical significance and biological role of TICRR in CM progression were assessed in this study.

Materials and Methods

Data Retrieval and Analysis

We downloaded TICRR expression profiles from the UCSC XENA Project (https://xenabrowser.net/datapages/), which contains the cancer genome atlas (TCGA) and Genotype Tissue Expression (GTEx) clinical pan-cancer data. 472 CM samples from TCGA were divided into two groups according to the median TICRR expression (low- and high-TICRR expression groups). The "DESeq2" R package was used to identify database differentially expressed genes (DEGs) between the two groups. Then we used the "clusterProfiler" and "ggplot2" R packages to analyse and visualise the functions of identified DEGs, including Gene Ontology (GO), Kyoto Encyclopedia of Genes and Genomes (KEGG), and gene set enrichment analysis (GSEA). To evaluate the prognostic role of TICRR in CM, the Kaplan-Meier survival curve, nomogram model and risk score curve were established. Univariate and multivariate Cox regression analyses were conducted to identify the candidates for the nomogram construction. In addition, immune cell infiltration and Spearman analysis were performed to determine the relationship between TICRR expression and immune cell infiltration.

Tissue Samples and Ethics Statement

To further verify the difference in TICRR expression between CM and normal skin, six pairs of tumour tissues and human normal skin (HNS) tissues were collected and divided into two parts: one was paraffin-embedded for immunohistology, the other was stored in liquid nitrogen for further experiments. This study followed the Helsinki Declaration and received approval from the Ethics Committee Board of the Second People's Hospital of Yibin. Informed consent has been obtained from all individuals included in this study.

Cell Culture

Human CM cell lines (A375, A2058) were purchased from iCell Bioscience Inc. (Shanghai, China). All cell lines were cultured in Dulbecco's Modified Eagle Medium (DMEM; Gibco, USA) supplemented with 10% fetal bovine serum (FBS; Gibco, USA) at 37°C with 5% CO2.

Lentiviral Vector Construction and Generation of Stable Cell Lines

TICRR-knockdown lentivirus (Sh-TICRR) and its negative control lentivirus (Sh-Control), TICRR-overexpressing lentivirus (OE-TICRR) and its negative control lentivirus (OE-Control) were purchased from VectorBuilder Inc. (Guangdong, China). Cells were infected with lentivirus using polybrene (GeneChem, Shanghai, China) according to the manufacturer's instructions. After 72 hours of infection, two ug/mL puromycin was used to select stable clonal cell lines. The sequence of shRNA was listed in Table S1.

RNA Extraction and Quantitative Real-Time Reverse Transcription PCR (q-PCR)

Total RNA was isolated using a TRIzol reagent (Takara, Japan). All primers used for q-PCR were obtained from ServiceBio (Wuhan, China). The primer sequences were (5'-3'): TICRR forward -ATCCTGGTCCTGATATTGGTGTT, reverse -TTTGGTCTGACTTATCTTGCTGG. GAPDH forward -GGAAGCTTGTCATCAATGGAAATC, reverse -TGATGACCCTTTTGGCTCCC. GAPDH was used as the internal control, and the relative expression levels of TICRR were calculated according to the 2-ΔΔCT method.

Cell Viability Assay

Each experimental group of cells in the logarithmic growth phase was trypsinised, resuspended in a complete medium, and cultured overnight. According to the manufacturer's protocol, Cell Counting KIT-8 reagent (Abcam, USA) was used for the next four days to assess cell viability. Finally, the optical density at 462 nm at each time point was detected by a microplate reader.

Flow Cytometry (FCM) Assays

Cells were fixed with 70% ethanol when the fusion rate reached 80%. Subsequently, A375 cells were washed and incubated in the dark at 4°C with PI/RNase staining buffer on ice overnight. The fluorescence of individual nuclei was analysed on a BD LSRFortessa analyser (BD Biosciences, Franklin Lakes, USA).

Scratch Assays

Cells were plated in six-well plates and cultivated until 90% confluence. The scratch was created with a 200ul sterilised pipette tip. Following the removal of debris, serum-free DMEM was added. We then obtained three randomly selected images from each well using a microscope at 0h/24h/48h, respectively. The scratch areas at 0 h were set as 100%, and the migration rates at various time points were compared.

Transwell Assays

Cells were harvested, resuspended in serum-free medium, and then plated in the upper chamber of transwell (Corning, NY, USA) for migration assays or plated in the upper chamber coated with Matrigel (Corning, NY, USA) for invasion assays. The complete medium with 10% FBS was added to the lower chamber and incubated for 24h at 37°C. After that, cells were wiped from the top surface of the chamber. Cells on the bottom surface were fixed with 4% paraformaldehyde for 10 minutes and stained with crystal violet (Servicebio, Wuhan, China) for 5 minutes. The number of migrating or invading cells was imaged and counted.

Immunohistochemical (IHC) Staining

The paraffin-embedded tissues mentioned above were sectioned, followed by deparaffinisation and rehydration. Subsequently, EDTA was used for antigen repair. After that, the slides were incubated with primary antibody at 4°C overnight. On the second day, the slides were incubated with a secondary antibody for 1h at 37°C. Image acquisition was done using a digital pathology section scanner (Kfbio, Ningbo, China). Antibodies used in the experiment were listed in Table S2.

Immunofluorescence (IF)

A375 cells were seeded in 48-well dishes and cultured to 80% confluence. Then, cell samples were fixed in 4% paraformaldehyde for 15 minutes at room temperature. Cell samples and tissue sections were washed, permeabilised, and blocked. We used corresponding antibodies to investigate protein expression. Images were captured using a confocal microscope (Zeiss, Oberkochen, Germany). Antibodies used in the experiment were listed in Table S3.

Statistical Analysis

Data were depicted as means ± standard derivation ($\bar{x} \pm s$). All continuous variables have gone through the Kolmogorov–Smirnov Test. Normally distributed variables were analysed using an independent-samples *t*-test (Levene's test for equality of variances, if necessary). All data analyses were carried out using the GraphPad Prism software (9.0, USA). Two-tailed P values < 0.05 were considered significant. Each experiment was performed at least in triplicate.

Results

TICRR Was Overexpressed in Pan-Cancer and CM

Based on TCGA and GTEx databases, we analysed the expression levels of TICRR in thirty-three pan-cancer samples. Among them, twenty-four cancers showed higher expression of TICRR than the corresponding normal tissues, and only

three cancers showed lower expression of TICRR (Figure 1a). Specifically, a significant up-regulation of TICRR was found in CM compared to HNS tissues (Figure 1b). We collected six CM and six HNS samples from our hospital for q-PCR, IHC and IF analysis to verify the bioinformatics results further. It was found that the expression of TICRR in CM tissues was significantly up-regulated at both mRNA and protein levels (Figure 1c–g).

Overexpressed TICRR Predicted a Worse Prognosis in CM Patients

We constructed Kaplan-Meier survival curves and found that patients with high expression of TICRR had worse overall survival (OS) and disease-specific survival (DSS) compared to those patients with low expression of TICRR (Figure 1h

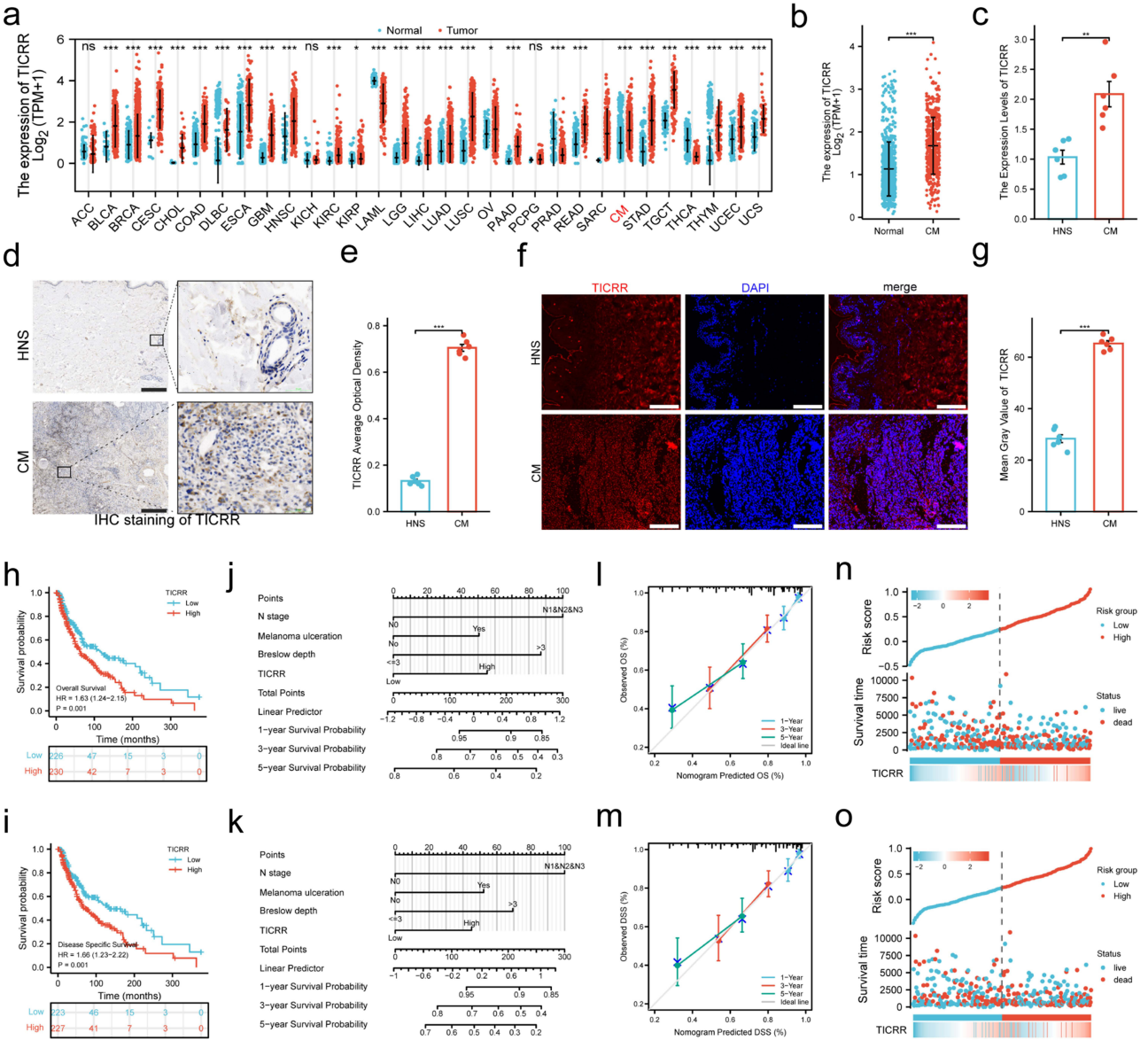

Figure 1 TICRR was overexpressed in CM and associated with worse prognostic value. **(a)** TICRR was highly expressed in most cancer species, including CM. **(b)** Comparison of mRNA levels of TICRR in CM and HNS tissues from TCGA and GTEx databases. **(c)** mRNA levels of TICRR in collected samples (n = 6). **(d and e)** Representative images of TICRR immunohistochemistry and corresponding quantification in collected CM and HNS tissues (n = 6; scale bar = 500 μm). **(f and g)** Representative pictures of TICRR immunofluorescence and corresponding quantification in collected CM and HNS tissues (n=6; scale bar=200 μm). **(h and i)** Kaplan-Meier analysis of OS **(h)** and DSS **(i)** in CM patients with different TICRR expression levels. **(j and k)** Nomogram model predicting the 1-year, 3-year, 5-year OS **(j)** and DSS **(k)** of patients with CM. **(l and m)** Calibration chart evaluating the predictive accuracy of the nomogram. **(n and o)** Risk score curve showing TICRR expression, OS status **(n)**, DSS status **(o)**, and risk score. ns, $P \geq 0.05$; **, $P < 0.01$; ***, $P < 0.001$.

Abbreviations: (CM, cutaneous melanoma; HNS, human normal skin; TCGA, the Cancer Genome Atlas; GTEx, Genotype Tissue Expression; OS, overall survival; DSS, disease-specific survival).

and i). According to the univariate and multivariate Cox proportional hazards analysis, the expression of TICRR, clinical N stage, melanoma ulceration, and Breslow depth were independent risk factors for OS in CM (Table 1). Meanwhile, TICRR expression, clinical N stage, and Breslow depth were independent risk factors for DSS in CM (Table 2). We also established prognostic nomograms based on the significant OS/DSS prognostic indicators created in Cox regression analysis. In addition, the high expression of TICRR contributed nearly 60 points to the total points, suggesting that TICRR played an essential role in the prognosis of CM patients (Figure 1j and k). Moreover, calibration plots were also constructed to evaluate the prediction accuracy of the two nomograms. The prediction of the two nomograms was highly consistent with the actual survival results, except that the 5-year prediction was slightly overestimated (Figure 1l and m). Finally, risk score curves showed that the expression of TICRR was negatively associated with OS/DSS time and positively correlated with risk score (Figure 1n and o). All the above results illustrated that overexpressed TICRR was correlated with a poor prognosis in CM patients.

Table 1 Univariate and Multivariate Cox Proportional Hazards Analysis of TICRR Expression and OS for CM Patients

Characteristics	Univariate Analysis		Multivariate Analysis	
	Hazard Ratio (95% CI)	P Value	Hazard Ratio (95% CI)	P Value
T stage (T1&T2 vs T3&T4)	2.085 (1.501–2.895)	**<0.001**	1.043 (0.593–1.834)	0.884
N stage (N0 vs N1&N2&N3)	1.752 (1.304–2.354)	**<0.001**	4.531 (1.342–15.295)	**0.015**
M stage (M0 vs M1)	1.897 (1.029–3.496)	**0.040**	2.245 (0.848–5.943)	0.104
Age (≤60 vs.>60)	1.656 (1.251–2.192)	**<0.001**	0.941 (0.625–1.416)	0.770
Gender (Female vs Male)	1.172 (0.879–1.563)	0.281		
Pathologic stage (I&II vs III&IV)	1.617 (1.207–2.165)	**0.001**	0.477 (0.138–1.644)	0.241
Melanoma ulceration (No vs Yes)	2.085 (1.495–2.907)	**<0.001**	1.529 (1.011–2.313)	**0.044**
Melanoma Clark level (I&II&III vs IV&V)	2.167 (1.508–3.113)	**<0.001**	1.520 (0.933–2.474)	0.093
BMI (≤25 vs >25)	0.827 (0.513–1.333)	0.436		
Breslow depth (≤3 vs >3)	2.651 (1.938–3.627)	**<0.001**	2.048 (1.209–3.468)	**0.008**
Radiation therapy (No vs Yes)	0.977 (0.694–1.377)	0.895		
TICRR (Low vs High)	1.305 (1.106–1.540)	**0.002**	1.546 (1.202–1.990)	**<0.001**

Notes: Two-tailed P values < 0.05 were considered significant and exhibited in bold text.
Abbreviations: TICRR, TopBP1 interacting checkpoint and replication regulator; OS, overall survival; CM, cutaneous melanoma; T, tumour, N, node; M, metastasis; BMI, body mass index.

Table 2 Univariate and Multivariate Cox Proportional Hazards Analysis of TICRR Expression and DSS for CM Patients

Characteristics	Univariate Analysis		Multivariate Analysis	
	Hazard Ratio (95% CI)	P Value	Hazard Ratio (95% CI)	P Value
T stage (T1&T2 vs T3&T4)	1.887 (1.341–2.654)	**<0.001**	1.067 (0.600–1.898)	0.825
N stage (N0 vs N1&N2&N3)	1.665 (1.214–2.283)	**0.002**	6.476 (1.494–28.073)	**0.013**
M stage (M0 vs M1)	2.200 (1.190–4.069)	**0.012**	2.514 (0.939–6.729)	0.066
Age (≤60 vs.>60)	1.699 (1.258–2.294)	**<0.001**	0.938 (0.610–1.444)	0.772
Gender (Female vs Male)	1.161 (0.855–1.575)	0.340		
Pathologic stage (I&II vs III&IV)	1.536 (1.125–2.096)	**0.007**	0.334 (0.075–1.482)	0.149
Melanoma ulceration (No vs Yes)	1.948 (1.372–2.767)	**<0.001**	1.477 (0.958–2.279)	0.078
Melanoma Clark level (I&II&III vs IV&V)	2.128 (1.457–3.108)	**<0.001**	1.580 (0.947–2.634)	0.080
BMI (≤25 vs >25)	0.937 (0.545–1.612)	0.815		
Breslow depth (≤3 vs >3)	2.274 (1.628–3.177)	**<0.001**	1.799 (1.049–3.085)	**0.033**
Radiation therapy (No vs Yes)	0.994 (0.689–1.433)	0.973		
TICRR (Low vs High)	1.333 (1.119–1.590)	**0.001**	1.493 (1.145–1.945)	**0.003**

Notes: Two-tailed P values < 0.05 were considered significant and exhibited in bold text.
Abbreviation: DSS, disease-specific survival.

Identification of DEGs and Functional Enrichment Analysis

According to the median expression level of TICRR, 472 patients were divided into low- and high-TICRR groups. As shown in Figure 2a, with the thresholds of log FC > 1.5 and adjusted *P* value < 0.05, 484 DEGs (202 up-regulated and 282 down-regulated) were identified. A heat map showed the representative DEGs between the two groups (Figure 2b). GO and KEGG analysis showed that the functions of DEGs were mainly involved in cell cycle and DNA replication (Figure 2c–f). Subsequently, GSEA was performed to explore the potential mechanism of TICRR in CM pathogenesis. The results indicated that overexpression of TICRR was positively associated with cell cycle and pro-oncogenic pathways and negatively correlated with keratinisation (Figure 2g–i). These results suggested that overexpression of TICRR showed a worse outcome in part due to the active proliferation of tumour cells, the hyper-activation of pro-oncogenic pathways, and the inhibition of keratinisation.

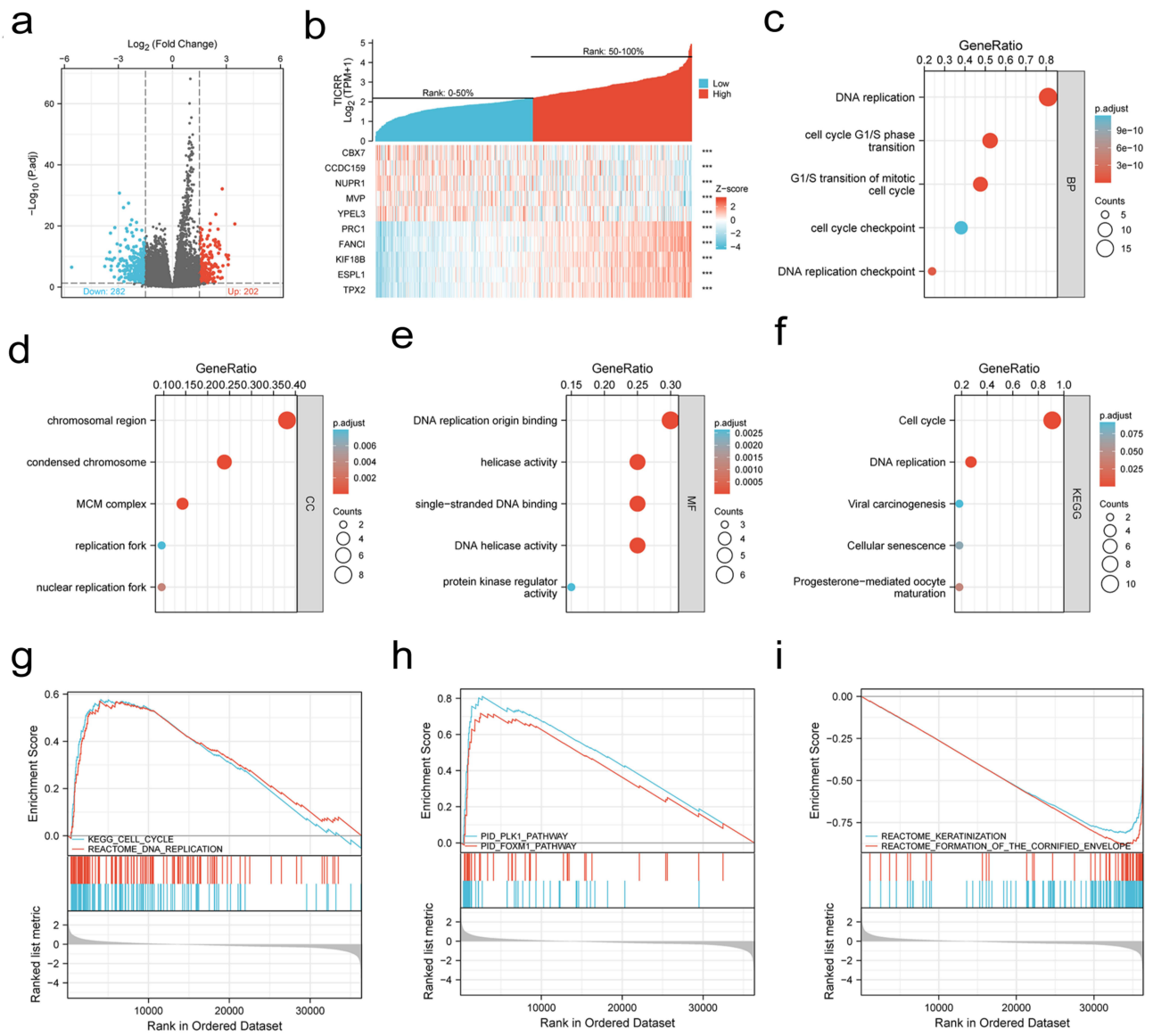

Figure 2 Identification of DEGs and functional enrichment analysis. **(a and b)** Volcano plots and heatmaps displaying expression profiles of DEGs in the two subgroups. **(c–e)** GO analysis of DEGs, including BP **(c)**, CC **(d)**, and MF **(e)**. **(f)** KEGG analysis of DEGs. **(g–i)** GSEA identified that TICRR positively correlated with the cell cycle **(g)** and pro-oncogenic pathways **(h)** and negatively correlated with keratinisation **(i)**.

Abbreviations: DEGs, differentially expressed genes; GO, gene oncology; BP, biological process; CC, cellular component; MF, molecular function; KEGG, Kyoto encyclopedia of genes and genomes; GSEA, gene set enrichment analysis.

Knockdown of TICRR Reduced the Proliferation of CM Cells in vitro

GSEA showed that high expression of TICRR was positively related to the cell cycle (Figure 3a). To further investigate the role of TICRR in CM cells, a lentivirus containing short hairpin RNA targeting TICRR (sh-TICRR) was constructed. q-PCR assays demonstrated that infection of sh-TICRR could efficiently reduce the expression of TICRR in A375 and A2058 cell lines (Figure 3b). CCK8 assays showed that TICRR silencing potently interfered with cell viability in A375 and A2058 cells (Figure 3c and d). Immunofluorescence also indicated that TICRR silencing dramatically reduced the expression of Ki67 in A375 and A2058 cells, indicating that the knockdown of TICRR suppressed the proliferation of CM cells (Figure 3e and f). Furthermore, the FCM assay of the cell cycle demonstrated that TICRR silencing inhibited A375 and A2058 cell proliferation by prolonging the G0/G1 phase and shortening the G2/M phase, suggesting that TICRR participated significantly in CM cell proliferation (Figure 3g and h). All the results illustrated that TICRR was an essential positive regulator of proliferation in CM. Furthermore, silencing of TICRR may arrest the proliferation of CM cells.

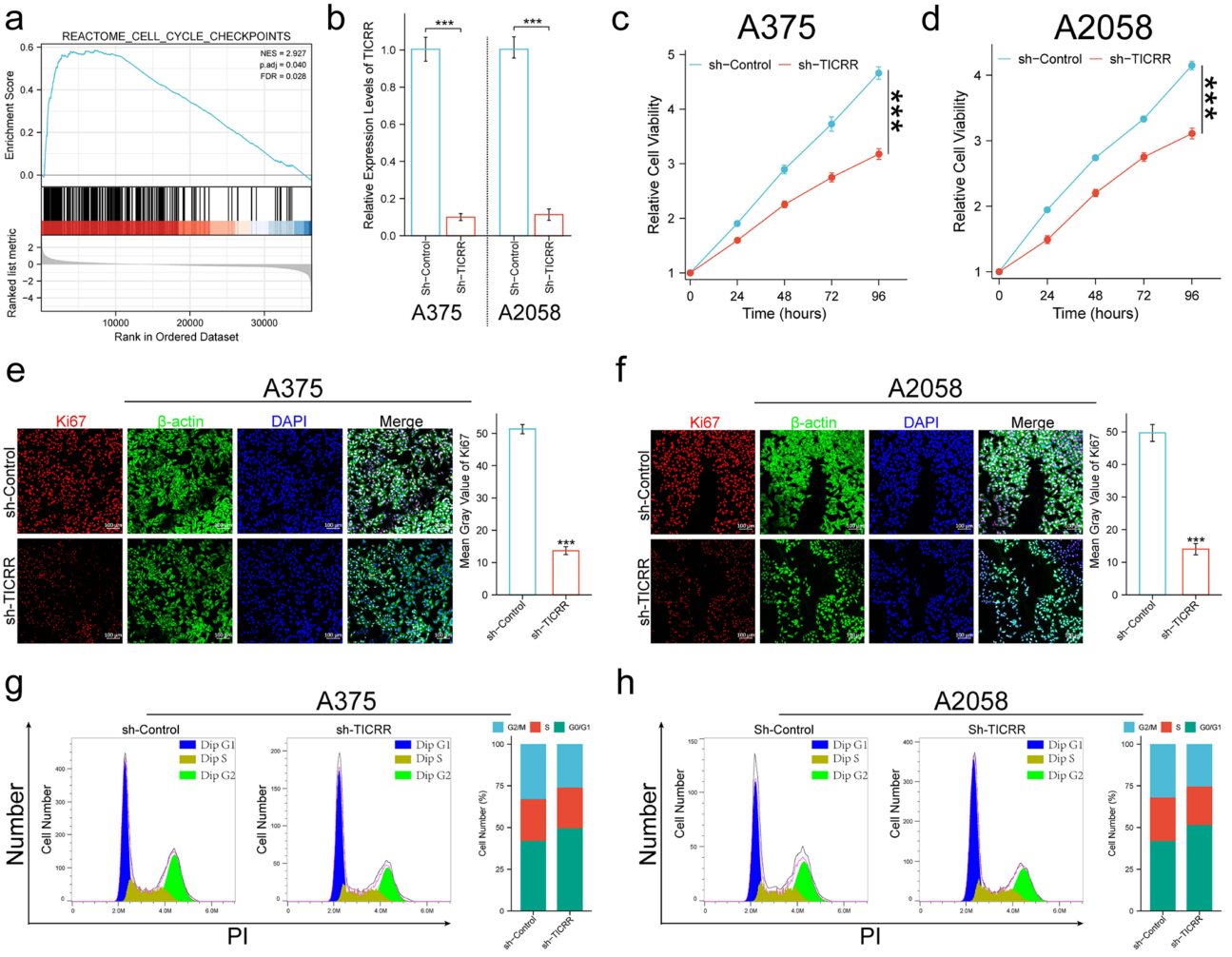

Figure 3 Knockdown of TICRR reduced the proliferative ability of CM cells in vitro. CM cell lines (A375 and A2058) were infected with TICRR-knockdown lentivirus (sh-TICRR) or corresponding control lentivirus (sh-Control). **(a)** GSEA identified that high TICRR expression was positively correlated with the cell cycle. **(b)** The establishment of sh-TICRR stable cell lines was verified at the mRNA level. **(c and d)** CCK8 assays of A375 **(c)** and A2058 cells **(d)** with TICRR silencing or not. (e-f) Ki-67 immunocytochemistry and corresponding quantification of A375 (e) and A2058 cells (f) with TICRR silencing or not (scale bar = 100 μm). **(g and h)** Flow cytometry of PI staining and quantification in A375 **(g)** and A2058 cells **(h)** with TICRR silencing. ***, $P < 0.001$.

Knockdown of TICRR Inhibited the Migration and Invasion Capabilities of CM Cells

GSEA identified that high expression of TICRR was negatively correlated with cell adhesion (Figure 4a). To confirm this result, scratch assays, transwell migration and matrigel invasion assays were performed to determine CM cells' migration and invasion capacities under different TICRR expression levels. The results of scratch assays showed that TICRR silencing interfered with cell migration in A375 and A2058 cells (Figure 4b and c). Transwell migration assays also indicated that TICRR silencing dramatically reduced the number of migrating cells, indicating that knockdown of TICRR suppressed the migration of CM cells (Figure 4d and e). Furthermore, cell invasion ability was detected using matrigel-coated transwell chambers. The results showed that TICRR silencing also decreased the number of invading cells, suggesting that knockdown of TICRR suppressed the invasion of CM cells (Figure 4f and g). These findings indicated that TICRR may be pivotal in regulating CM cells' migratory and invasive capacities.

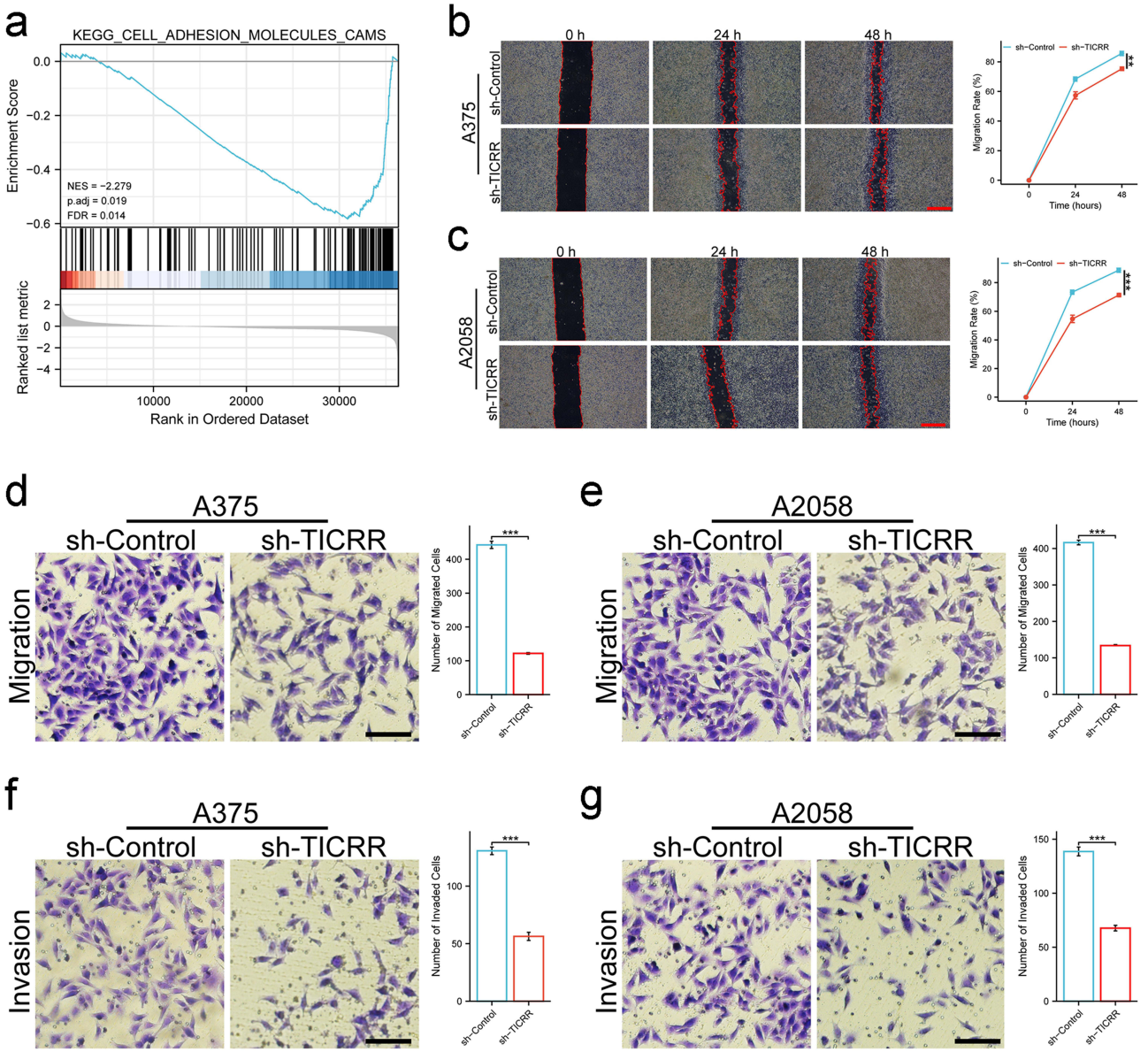

Figure 4 Knockdown of TICRR inhibited CM cells' migration and invasion capabilities in vitro. **(a)** GSEA identified that high TICRR expression was negatively correlated with cell adhesion. **(b and c)** The migration ability of A375 **(b)** and A2058 cells **(c)** with different TICRR levels was determined with the scratch assay (scale bar = 200 μm). **(d and e)** The migration ability of A375 **(d)** and A2058 cells **(e)** with different TICRR levels was also detected by transwell assay (scale bar = 100 μm). **(f and g)** The invasion capability of A375 **(f)** and A2058 cells **(g)** with different TICRR levels was detected using matrigel-coated transwell cell culture chambers (scale bar = 100 μm). **, $P < 0.01$; ***, $P < 0.001$.

TICRR Promoted CM Aggressiveness by Activating the PI3K/AKT/mTOR Signalling Pathway

GSEA identified that high expression of TICRR was negatively correlated with negative regulation of the PI3K/AKT network, suggesting that TICRR could activate this signalling pathway (Figure 5a). The PI3K/Akt/mTOR signalling has been demonstrated to be associated with cell proliferation and invasion. Therefore, we hypothesised that TICRR could promote CM aggressiveness via activating the PI3K/AKT/mTOR pathway. Rescue experiments were conducted to verify whether TICRR overexpression potentiated CM cells' aggressiveness by activating the PI3K/AKT/mTOR pathway. Specifically, stable TICRR-overexpression cell lines were constructed via lentiviral infection (OE-TICRR). Then, we treated the two stable cell lines overexpressing TICRR with LY294002, a PI3K/AKT pathway inhibitor. CCK8 assays confirmed that the proliferation of A375 and A2058 cells significantly increased following TICRR overexpression, while LY294002 treatment partially offset the pro-proliferation effect of TICRR (Figure 5b and c). Meanwhile, Transwell migration and matrigel invasion assays suggested that migrating or invading cells remarkably increased following TICRR overexpression. At the same time, the potentiation effects of TICRR were partially counteracted by LY294002 treatment, implying that TICRR promoted the aggressiveness of CM, at least in part, via activation of the PI3K/AKT/mTOR signalling. (Figure 5d and e).

TICRR Expression Was Correlated with Immune Infiltration Levels

Since the effectiveness of immunotherapy was linked to the infiltration of immune cells in the tumour microenvironment (TME), we scored the enrichment of 24 immune cells using the ssGSEA method. The results showed that TICRR was positively correlated with the infiltration of Th2 cells (r=0.283; P<0.001), while negatively associated with the infiltration of pDC (r=−0.293; P<0.001), Treg (r=−0.275; P<0.001), cytotoxic cells (r=−0.263; P<0.001), DC (r=−0.261; P<0.001), neutrophils (r=−0.254; P<0.001) in CM (Figure 6a–c). As immune checkpoints were key regulators of T cell activation and immune cell infiltration, we next determined the landscape of checkpoint expression in the TME of CM. The radargram showed that TICRR was closely associated with the molecular targets of CM, including BRAF, CD276, NF1, NRAS and KRAS (Figure 6d). Finally, immunofluorescence and quantitative analysis revealed that TICRR was highly co-expressed with CD4 in CM tissues compared with HNS tissues (Figure 6e and f). These results showed that the expression of TICRR had a close association with TME and immunotherapy response in CM.

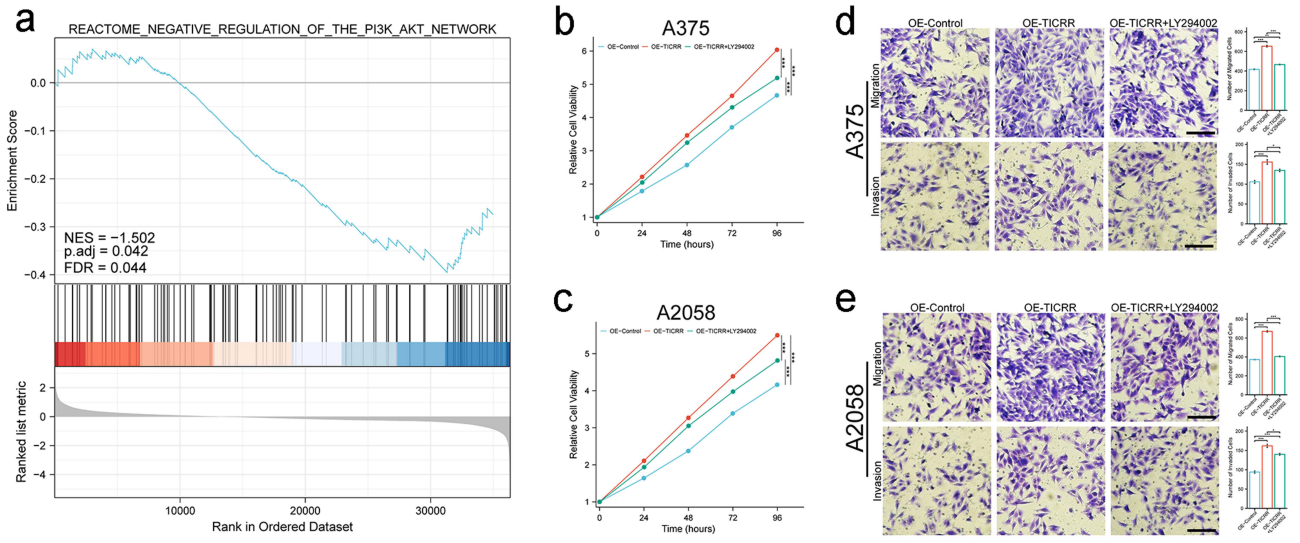

Figure 5 TICRR promoted CM aggressiveness through activating the PI3K/AKT/mTOR pathway. Cells were infected with TICRR overexpression lentivirus (OE-TICRR), corresponding control lentivirus (OE-Control), or cells overexpressing TICRR were treated with LY294002, a PI3K/AKT inhibitor. **(a)** GSEA identified that TICRR was positively correlated with the PI3K/AKT signalling pathway. **(b and c)** CCK-8 assay assessed the proliferation ability of A375 **(b)** and A2058 **(c)** cells. **(d and e)** The migration and invasive abilities of A375 **(d)** and A2058 **(e)** cells were determined by transwell migration and matrigel invasion assays (scale bar = 100 μm). ns, $P \geq 0.05$; **, $P < 0.01$; ***, $P < 0.001$.

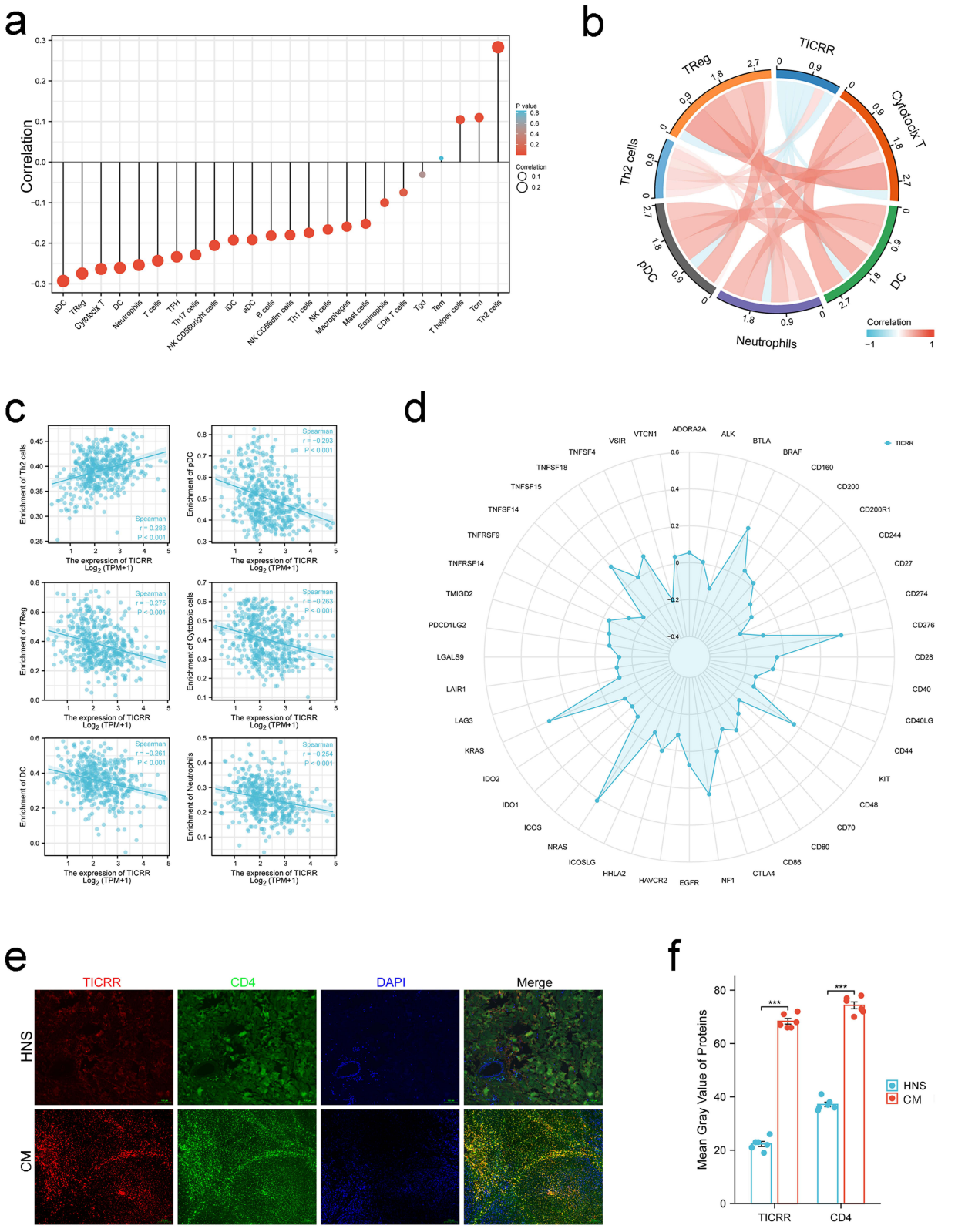

Figure 6 TICRR is closely related to the infiltration of immune cells in the tumour microenvironment. **(a)** Lollipop diagram showing the correlation between TICRR and infiltration of immune cells. **(b)** Chord plot showing the relationship between TICRR and top 5 TICRR-associated immune cells. **(c)** Scatter plots verifying the correlation between TICRR and infiltration of immune cells. **(d)** Radargram shows the relationship between TICRR and immune checkpoint genes as well as chemokines/chemokine receptors. **(e and f)** Representative immunofluorescence images and quantitative analysis suggested that both TICRR and CD4 were overexpressed in CM (n = 6). ***, $P < 0.001$.

Discussion

While tremendous progress has been made in the past ten years in improving the outcomes of CM, it remains the most lethal skin cancer worldwide.[3,15] Therefore, it is imperative to investigate the underlying mechanisms and identify novel diagnostic and therapeutic targets for CM. TICRR, as an essential regulator of DNA replication initiation, has a level and phosphorylation that determine the number of S-phase origins. Typically, intracellular levels of TICRR are high in the G1 phase, whereas TICRR levels decline sharply when cells enter the S phase and begin DNA replication.[16] Thus, continuously elevated TICRR in pathological conditions affects the cell cycle and may affect the progression of carcinomas.

To investigate the role of TICRR in CM, we identified 484 DEGs and performed a functional enrichment analysis in the study. Several cell cycle-related pathways and oncogenic-related pathways were positively correlated with TICRR expression. In contrast, keratinisation negatively correlated with TICRR expression, indicating that TICRR promoted tumour cell proliferation and significantly inhibited skin keratinisation. Consistently, previous studies have shown that each melanocyte is in contact with about 30 keratinocytes to form the epidermal-melanin unit in normal skin, which is essential for melanocyte homeostasis.[17–19] However, functional enrichment results in the study revealed that the expression of TICRR in CM was negatively correlated with keratinisation. This may break the melanocyte homeostasis and thereby affect CM prognosis.

Previous studies have verified that the knockdown of TICRR significantly inhibited the proliferation of tumour cells in both breast cancer and hepatocellular carcinoma.[11,20] In the present study, the proliferation, migration, and invasion of CM cells were dramatically inhibited when TICRR was silenced, and overexpression of TICRR produced the opposite effect, both consistent with the prediction of bioinformatics analysis results. Furthermore, it was confirmed that TICRR was closely related to immune cell infiltration activities using immune infiltration and immunofluorescence analysis.

Though the underlying mechanism was yet to be elucidated, the PI3K/AKT signalling pathway has been proven vital in promoting tumorigenicity and metastasis in cancer.[2,21] As reported before, mitogen-activated protein kinase (MAPK) is the most frequently dysregulated pathway in CM, and the second most frequently activated pathway is the PI3K/AKT pathway, which plays a crucial role in maintaining cellular homeostasis.[2] Consistent with previous studies, we also found that the knockdown of TICRR inhibited the phosphorylation of critical molecules in the PI3K/AKT signalling pathway, which may be the underlying mechanism that TICRR participate in CM progression.[22,23] Meanwhile, the radargram in the present study showed that TICRR was closely associated with the molecular targets of CM, including BRAF, NF1, KIT, NRAS and KRAS, all of which have been validated to be correlated with CM before.[2] BRAF-targeted therapy has been applied in the clinical treatment of CM and showed favourable outcomes in the overall survival rate.[7] The NF1 protein serves as a regulator of the RAS family, and loss-of-function mutations in NF1 result in an activated PI3K/AKT signalling pathway through the hyperactivation of NRAS. The receptor tyrosine kinase KIT also activates PI3K, and the MAPK signalling cascades, affecting the proliferation and survival of melanoma cells. Moreover, TICRR suppression substantially attenuated the activation of PI3K/AKT/mTOR signalling, while the PI3K/AKT inhibitor could partially reverse the aggressiveness-enhancing effect induced by TICRR overexpression. The results indicated that the PI3K/AKT/mTOR pathway might participate in the TICRR-mediated CM cell's aggressiveness.

As for the relationship between TME and TICRR expression, immune cells were involved in manipulating TME components and the progression of tumours from all stages of tumorigenesis.[24,25] Our results showed that TICRR expression was associated with the infiltration of various immune cells in CM, including Th1/Th2 cells, Tregs, cytotoxic T lymphocytes, dendritic Cells (DCs), plasmacytoid dendritic cells (pDCs) and neutrophils. DCs and pDCs, as the critical cells for antigen presentation, play a crucial role in tumour immunity.[26,27] However, we found that the infiltration levels of these two immune cells were negatively correlated with TICRR expression. Cytotoxic T lymphocytes could easily kill tumour cells presented by DCs.[28] TICRR also inhibit cytotoxic T lymphocyte infiltration in the TME, which counteracts the cancer cells, eliminating the effect of cytotoxic T lymphocytes.[29] Moreover, our results showed that TICRR was positively correlated with Th2 infiltration level but negatively correlated with Th1 infiltration level. The "Th1/Th2 drift" caused by high expression of TICRR might be responsible for the poor prognosis of CM patients.[30,31]

Conclusion

In summary, we identified for the first time that TICRR is overexpressed in CM, and this high expression correlates with poor prognosis of CM patients. Down-regulating TICRR expression could significantly reduce the proliferation, migration, and invasion of CM cells. We also found that the PI3K/AKT/mTOR pathway might participate in the TICRR-mediated CM cell's aggressiveness. Furthermore, TICRR was proved to be closely related to the infiltration of immune cells in TME, further suggesting TICRR was a potential therapeutic target of CM.

Abbreviation

TopBP1 interacting checkpoint and replication regulator, TICRR; cutaneous melanoma, CM; the Cancer Genomic Atlas, TCGA; differentially expressed genes, DEGs; gene ontology, GO; Kyoto Encyclopedia of Genes and Genomes, KEGG; gene set enrichment analysis, GSEA; human normal skin, HNS; overall survival, OS; disease-specific survival, DSS; tumour microenvironment, TME.

Data Sharing Statement

All data generated or analysed during this study are included in this published article. The datasets used and/or analysed during the present study are available from the corresponding author upon reasonable request.

Ethical Approval

The research related to human use has complied with all the relevant national regulations and institutional policies and in accordance with the tenets of the Helsinki Declaration and has been approved by the Ethics Committee Board of the Second People's Hospital of Yibin (No. 2024-012-01).

Funding

This research received no specific grant from funding agencies in the public, commercial, or not-for-profit sectors.

Disclosure

The authors have no relevant financial or non-financial interests to disclose in this work.

References

1. Long GV, Swetter SM, Menzies AM, Gershenwald JE, Scolyer RA. Cutaneous melanoma. *Lancet*. 2023;402(10400):485–502. doi:10.1016/s0140-6736(23)00821-8
2. Gosman LM, Țăpoi DA, Costache M. Cutaneous melanoma: a review of multifactorial pathogenesis, immunohistochemistry, and emerging biomarkers for early detection and management. *Int J Mol Sci*. 2023;24(21):15881. doi:10.3390/ijms242115881
3. Arnold M, Singh D, Laversanne M, et al. Global burden of cutaneous melanoma in 2020 and projections to 2040. *JAMA Dermatol*. 2022;158(5):495–503. doi:10.1001/jamadermatol.2022.0160
4. Teixido C, Castillo P, Martinez-Vila C, Arance A, Alos L. Molecular markers and targets in melanoma. *Cells*. 2021;10(9):2320. doi:10.3390/cells10092320
5. Thielmann CM, Chorti E, Matull J, et al. NF1-mutated melanomas reveal distinct clinical characteristics depending on tumour origin and respond favourably to immune checkpoint inhibitors. *Eur J Cancer*. 2021;159:113–124. doi:10.1016/j.ejca.2021.09.035
6. He Z, Chen M, Luo Z. Identification of immune-related genes and integrated analysis of immune-cell infiltration in melanoma. *Aging*. 2024;16(1):911–927. doi:10.18632/aging.205427
7. Leonardi GC, Falzone L, Salemi R, et al. Cutaneous melanoma: from pathogenesis to therapy (Review). *Int J Oncol*. 2018;52(4):1071–1080. doi:10.3892/ijo.2018.4287
8. Can G, Kauerhof AC, Macak D, Zegerman P. Helicase subunit Cdc45 targets the checkpoint kinase Rad53 to both replication initiation and elongation complexes after fork stalling. *Mol Cell*. 2019;73(3):562–573.e3. doi:10.1016/j.molcel.2018.11.025
9. Di Micco R, Fumagalli M, Cicalese A, et al. Oncogene-induced senescence is a DNA damage response triggered by DNA hyper-replication. *Nature*. 2006;444(7119):638–642. doi:10.1038/nature05327
10. Kumagai A, Shevchenko A, Shevchenko A, Dunphy WG. Treslin collaborates with TopBP1 in triggering the initiation of DNA replication. *Cell*. 2010;140(3):349–359. doi:10.1016/j.cell.2009.12.049
11. Yu Q, Pu SY, Wu H, et al. TICRR contributes to tumorigenesis through accelerating DNA replication in cancers. *Front Oncol*. 2019;9:516. doi:10.3389/fonc.2019.00516
12. Xia S, Lin Y, Lin J, Li X, Tan X, Huang Z. Increased expression of TICRR predicts poor clinical outcomes: a potential therapeutic target for papillary renal cell carcinoma. *Front Genet*. 2020;11:605378. doi:10.3389/fgene.2020.605378

13. He KJ, Zhang YF, Liang LY, et al. ncRNAs-mediated high expression of TICRR promotes tumor cell proliferation and migration and is correlated with poor prognosis and tumor immune infiltration of hepatocellular carcinoma. *Mol Ther Nucleic Acids*. 2022;30:80–94. doi:10.1016/j.omtn.2022.09.007
14. Zheng X, Han L, Guan J, et al. TICRR serves as a prognostic biomarker in lung adenocarcinoma with implications in RNA epigenetic modification, DDR pathway, and RNA metabolism. *Front Oncol*. 2023;13:1274439. doi:10.3389/fonc.2023.1274439
15. Weiss SA, Wolchok JD, Sznol M. Immunotherapy of melanoma: facts and hopes. *Clin Cancer Res*. 2019;25(17):5191–5201. doi:10.1158/1078-0432.Ccr-18-1550
16. Wittig KA, Sansam CG, Noble TD, Goins D, Sansam CL. The CRL4DTL E3 ligase induces degradation of the DNA replication initiation factor TICRR/TRESLIN specifically during S phase. *Nucleic Acids Res*. 2021;49(18):10507–10523. doi:10.1093/nar/gkab805
17. Haass NK, Smalley KS, Li L, Herlyn M. Adhesion, migration and communication in melanocytes and melanoma. *Pigment Cell Res*. 2005;18(3):150–159. doi:10.1111/j.1600-0749.2005.00235.x
18. Scatolini M, Patel A, Grosso E, et al. GJB5 association with BRAF mutation and survival in cutaneous malignant melanoma. *Br J Dermatol*. 2022;186(1):117–128. doi:10.1111/bjd.20629
19. Zhao S, Wen S, Liu H, et al. High expression of TIMELESS predicts poor prognosis: a potential therapeutic target for skin cutaneous melanoma. *Front Surg*. 2022;9:917776. doi:10.3389/fsurg.2022.917776
20. Zhou Y, Lei D, Hu G, Luo F. A cell cycle-related 13-mRNA signature to predict prognosis in hepatocellular carcinoma. *Front Oncol*. 2022;12:760190. doi:10.3389/fonc.2022.760190
21. Wu S, Chen M, Huang J, et al. ORAI2 promotes gastric cancer tumorigenicity and metastasis through PI3K/Akt signaling and MAPK-dependent focal adhesion disassembly. *Cancer Res*. 2021;81(4):986–1000. doi:10.1158/0008-5472.Can-20-0049
22. Huang Y, Zhang J, Hou L, et al. LncRNA AK023391 promotes tumorigenesis and invasion of gastric cancer through activation of the PI3K/Akt signaling pathway. *J Exp Clin Cancer Res*. 2017;36(1):194. doi:10.1186/s13046-017-0666-2
23. Sun F, Wang J, Sun Q, et al. Interleukin-8 promotes integrin β3 upregulation and cell invasion through PI3K/Akt pathway in hepatocellular carcinoma. *J Exp Clin Cancer Res*. 2019;38(1):449. doi:10.1186/s13046-019-1455-x
24. Vitale I, Shema E, Loi S, Galluzzi L. Intratumoral heterogeneity in cancer progression and response to immunotherapy. *Nat Med*. 2021;27(2):212–224. doi:10.1038/s41591-021-01233-9
25. Hanahan D, Coussens LM. Accessories to the crime: functions of cells recruited to the tumor microenvironment. *Cancer Cell*. 2012;21(3):309–322. doi:10.1016/j.ccr.2012.02.022
26. Reizis B. Plasmacytoid dendritic cells: development, regulation, and function. *Immunity*. 2019;50(1):37–50. doi:10.1016/j.immuni.2018.12.027
27. Wculek SK, Cueto FJ, Mujal AM, Melero I, Krummel MF, Sancho D. Dendritic cells in cancer immunology and immunotherapy. *Nat Rev Immunol*. 2020;20(1):7–24. doi:10.1038/s41577-019-0210-z
28. Oh DY, Fong L. Cytotoxic CD4(+) T cells in cancer: expanding the immune effector toolbox. *Immunity*. 2021;54(12):2701–2711. doi:10.1016/j.immuni.2021.11.015
29. Weigelin B, den Boer AT, Wagena E, et al. Cytotoxic T cells are able to efficiently eliminate cancer cells by additive cytotoxicity. *Nat Commun*. 2021;12(1):5217. doi:10.1038/s41467-021-25282-3
30. Wu H, Zheng S, Zhang J, Xu S, Miao Z. Cadmium induces endoplasmic reticulum stress-mediated apoptosis in pig pancreas via the increase of Th1 cells. *Toxicology*. 2021;457:152790. doi:10.1016/j.tox.2021.152790
31. Zhang W, Pan Y, Gou P, et al. Effect of xanthohumol on Th1/Th2 balance in a breast cancer mouse model. *Oncol Rep*. 2018;39(1):280–288. doi:10.3892/or.2017.6094